Ordered phases in a bilayer system of dipolar fermions

B. P. van Zyl and W. Ferguson

Department of Physics, St. Francis Xavier University, Antigonish, Nova Scotia, Canada B2G 2W5
(Received 10 April 2016; published 24 May 2016)

The liquid-to-ordered phase transition in a bilayer system of fermions is studied within the context of our recently proposed density-functional theory [B. P. van Zyl, W. Kirkby, and W. Ferguson, Phys. Rev. A **92**, 023614 (2015)]. In each two-dimensional layer, the fermions interact via a repulsive, isotropic dipolar interaction. The presence of a second layer introduces an attractive *interlayer* interaction, thereby allowing the presence of inhomogeneous density phases which would otherwise be energetically unfavorable. For any fixed layer separation, we find an instability to a commensurate one-dimensional stripe phase in each layer, which always precedes the formation of a triangular Wigner crystal. However, at a certain *fixed* coupling, tuning the separation can lead to the system favoring a commensurate triangular Wigner crystal, or one-dimensional stripe phase, completely bypassing the Fermi liquid state. While other crystalline symmetries, with energies lower than the liquid phase can be found, they are never allowed to form owing to their high energetic cost relative to the triangular Wigner crystal and stripe phase.

I. INTRODUCTION

In a recent paper [1], a density-functional theory (DFT) [2] was developed for investigating the zero-temperature liquid-to-ordered phase transition in a single-component, two-dimensional (2D) dipolar Fermi gas (dFG). The model considered is one in which all of the dipoles are aligned perpendicular to the 2D xy plane, thereby rendering the dipole-dipole interaction isotropic and repulsive. The central finding of this study is that the single-layer dFG spontaneously breaks rotational invariance above some critical coupling to a one-dimensional stripe phase (1DSP), followed by a transition to a triangular Wigner crystal (TWC) at slightly higher coupling. The DFT prediction that the 1DSP precedes the formation of a 2D TWC is supported by earlier calculations utilizing the random-phase (RPA) [3–5], STLS (Singwi, Tosi, Land, and Sjolander) [6], and conserving Hartree-Fock (HF) approximations [7–10]. However, recent variational and quantum Monte Carlo (QMC) calculations [11–13] suggest that the TWC phase precedes the 1DSP with a coupling strength which is an order of magnitude larger than any of the values predicted in Refs. [1,3–10]. The controversy generated by the single-layer dFG studies suggests that it should also be interesting to consider the natural extension of this system to the case of two (or more) 2D layers.

To date, there are relatively few articles in the literature dealing with the density instabilities in multilayer systems. In Refs. [5,8,9], the RPA [5] and conserving HF [8,9] theoretical formulations were extended to the case of two or more layers, with a focus on investigating the instability toward a stripe phase in each layer. In these studies, when the intralayer dipolar interaction is purely repulsive, a transition to a 1DSP is found, with the stripes in each layer being "in-phase" (i.e., aligned with one another). An application of the STLS formalism to the multilayer case has also recently been provided in Refs. [14,15], where an in-phase 1DSP was found, along with the transition being shifted to lower coupling compared to the single-layer geometry. The consensus therefore appears to be that for repulsive intralayer dipolar interactions, a variation of the layer density and/or separation leads to the bilayer 2D dFG undergoing a transition to a 1DSP, such that the

stripes in each layer are commensurate or in phase. It is worthwhile pointing out that QMC calculations analogous to the single-layer dFG have yet to be performed for a multilayer configuration.

In this paper, we propose to extend the DFT of Ref. [1] to a bilayer 2D dFG, and investigate whether it predicts any additional density instabilities away from the uniform liquid state not present in the single-layer scenario. The motivation for this study is manifold. First, as mentioned above, there are a limited number of papers focusing on the quantum phase transition in a multilayer dFG, and of these studies, none have considered the possibility of a transition to a Wigner crystal. In addition, there is a complete absence of any application of DFT to the investigation of density instabilities in the bilayer dFG; filling this void will allow useful comparisons to be made with results obtained from other theoretical approaches [5,8,9,14,15], along with providing relevant predictions to be tested by any future QMC calculations on bilayer dipolar Fermi systems. Moreover, the mathematical formulation of DFT is exceedingly simple and computationally efficient, meaning that we are able to investigate a large set of system configurations with little additional effort. Finally, we are encouraged by the early work of Goldoni and Peeters [16], who implemented a DFT to examine the crystalline phases in a bilayer *electron* system. The result of their investigation was that the preferred ordered state in each layer is not necessarily the expected TWC. Specifically, depending on the layer separation and electronic density, the crystal phases could be square, rectangular, rhombic, or triangular. In fact, owing to the repulsive intralayer and interlayer Coulomb interactions, the crystalline structures in each 2D slab were found to be staggered relative to each other, so as to minimize the electrostatic energy of the system. Whether the bilayer 2D dFG possesses crystalline phases analogous to the bilayer 2D electron gas is certainly of interest, particularly in view of the fact that DFT predicts a 1DSP, rather than a TWC phase, as the preferred ordered state in the single-layer geometry.

To proceed, we organize the rest of our paper as follows. In Sec. II, we present the DFT appropriate to the bilayer 2D dFG, along with providing simple analytical results for
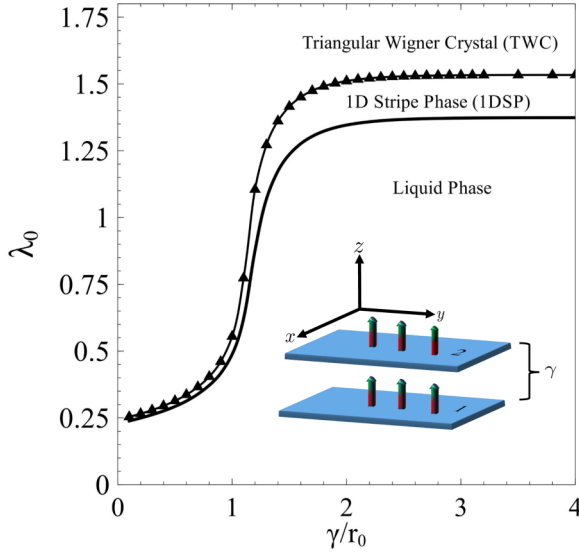
FIG. 1. Phase diagram of the bilayer system. As discussed in the text, λ_0 is the dimensionless coupling and r_0 is the dipolar length scale. For $\tilde{\gamma} = \gamma/r_0 \gtrsim 4$, the two layers are effectively uncoupled, and we reproduce the results found in Ref. [1]. The solid curve delineates the boundary between the liquid and 1DSP, while the solid curve with triangles separates the 1DSP from the TWC. The liquid $\rightarrow$ 1DSP and 1DSP $\rightarrow$ TWC are first-order phase transitions. Inset: A schematic depiction of the model under consideration. In each 2D layer, the atoms have their dipole moments (represented by the arrows) aligned with the z axis. The layers are separated by a distance γ.

examining the transition from the liquid-to-ordered state. Section III implements the results of Sec. II to generate

$$E_{SL}[\lambda(\mathbf{r})] = \frac{1}{16\pi} \frac{\hbar^2}{Mr_0^4} \int d^2r \lambda(\mathbf{r})^4 + \frac{\lambda_{vW}}{8\pi} \frac{\hbar^2}{Mr_0^2} \int d^2r |\nabla\lambda(\mathbf{r})|^2 + \frac{8}{45\pi^2} \frac{\hbar^2}{Mr_0^4} \int d^2r \lambda(\mathbf{r})^5 - \frac{C_{dd}}{4(4\pi)^2 r_0^4} \int d^2r \lambda(\mathbf{r})^2$$

$$\times \int d^2r' \int \frac{d^2k}{(2\pi)^2} k\, e^{-i\mathbf{k}\cdot(\mathbf{r}-\mathbf{r}')} \lambda(\mathbf{r}')^2 - \frac{1}{32\pi} \frac{\hbar^2}{Mr_0^4} \int d^2r \lambda(\mathbf{r})^6 \ln\left(1 + \frac{1}{a\sqrt{\lambda(\mathbf{r})} + b\lambda(\mathbf{r}) + c\lambda(\mathbf{r})^{\frac{3}{2}}}\right), \quad (2)$$

where $a = 1.1958, b = 1.1017$, and $c = -0.0100$ [13]. In Eq. (2), the first term is the Thomas-Fermi kinetic energy functional for a noninteracting Fermi system, the second term is the von Weizsäcker-like (vW) gradient correction to the kinetic energy [18], the third and fourth terms correspond to the LDA for the *total* dipole-dipole HF interaction energy (i.e., they *are not* separately the direct and exchange terms, respectively) [17,18], while the last term corresponds to the correlation energy [13]. Note that for a uniform system, $\rho(\mathbf{r}) \rightarrow \rho_0$ and the second and fourth terms in Eq. (2) vanish.

The total energy functional E_{SL} can then be used to investigate instabilities away from the Fermi liquid state by considering the quantity [19]

$$\Delta\varepsilon_{SL} = \varepsilon_{in} - \varepsilon_{un} = \frac{E_{SL}[\lambda(\mathbf{r})] - E_{SL}[\lambda_0]}{\int d^2r \rho_0} \left(\frac{\hbar^2}{Mr_0^2}\right)^{-1}, \quad (3)$$

which represents the *dimensionless* difference in energy (per particle) between the inhomogeneous and uniform phases. The

the phase diagram for the bilayer system. The paper closes in Sec. IV with our conclusions and suggestions for future work.

II. DFT FOR THE BILAYER 2D DFG

Let us briefly review some of the relevant mathematical and theoretical concepts necessary for the extension of the single-layer DFT [1] to a bilayer geometry. We recall that for a strictly 2D dFG with all of the moments oriented along the z axis (see the inset to Fig. 1), the dipole-dipole interaction is isotropic and repulsive, viz.,

$$V_{dd}(\mathbf{r} - \mathbf{r}') = \frac{C_{dd}}{4\pi |\mathbf{r} - \mathbf{r}'|^3}, \quad (1)$$

where $C_{dd} = \mu_0 d^2$ or $C_{dd} = p^2/\epsilon_0$, for magnetic (with magnetic moment d) or electric dipolar atoms (with electric dipole moment p), respectively. The vectors $\mathbf{r}$ and $\mathbf{r}'$ are the coordinates of two dipoles in the xy plane. The natural length and energy scales of the system are given by $r_0 = MC_{dd}/(4\pi\hbar^2)$ and $\hbar^2/Mr_0^2$, respectively, with M being the mass of an atom. Introducing the 2D Fermi wave vector, $k_F = \sqrt{4\pi\rho_0}$, we may define a dimensionless coupling constant (equivalently, density), viz., $\lambda_0 = k_F r_0$, where ρ_0 is the areal density of the uniform system. For a weakly inhomogeneous system, it is reasonable to introduce the local-density approximation (LDA) [2], which amounts to $\lambda_0 \rightarrow \lambda(\mathbf{r})$ and $k_F \rightarrow k_F(\mathbf{r})$; that is, in the LDA, the uniform density ρ_0 is replaced locally by a spatially varying density $\rho(\mathbf{r})$.

As discussed in detail in Ref. [1], the total energy functional for a single-layer (SL) 2D dFG (within the LDA) may be written as

results of applying Eq. (3) to various inhomogeneous densities are presented in Ref. [1], where it was found that the nonlocal contribution to the HF interaction energy, viz., the fourth term in Eq. (2), is crucial for the onset of a phase transition from the liquid to 1DSP. In other words, without the nonlocal term, the Fermi liquid state is always stable toward any ordered phase in the single-layer 2D dipolar Fermi gas.

The essential ingredient for extending Eq. (2) to the case of a bilayer system is the interlayer interaction energy between dipoles residing in different 2D slabs, viz.,

$$E_I[\rho] = \int d^2r \int d^2r' \rho_2(\mathbf{r}')V_I(\mathbf{r} - \mathbf{r}';\gamma)\rho_1(\mathbf{r}), \quad (4)$$

where $\rho_1(\mathbf{r})$ and $\rho_2(\mathbf{r}')$, and $\mathbf{r}$ and $\mathbf{r}'$, are the areal densities and spatial coordinates in layers 1 and 2, respectively (see the inset to Fig. 1). The interlayer interaction potential V_I reads

$$V_I(\mathbf{r} - \mathbf{r}';\gamma) = \frac{C_{dd}}{4\pi} \frac{|\mathbf{r} - \mathbf{r}'|^2 - 2\gamma^2}{(|\mathbf{r} - \mathbf{r}'|^2 + \gamma^2)^{5/2}}, \quad (5)$$

which is attractive for $|\mathbf{r} - \mathbf{r}'|^2 < 2\gamma^2$ and repulsive for $|\mathbf{r} - \mathbf{r}'|^2 > 2\gamma^2$, where γ is the separation between the two layers. Equation (4) is most easily evaluated by considering the Fourier transform of Eq. (5), viz.,

$$V_{\text{I}}(\mathbf{r} - \mathbf{r}'; \gamma) = \frac{1}{(2\pi)^2} \int d^2k\, \tilde{V}_{\text{I}}(\mathbf{k}; \gamma)\, e^{-i\mathbf{k}\cdot(\mathbf{r}-\mathbf{r}')}$$
$$= -\frac{C_{\text{dd}}}{2} \frac{1}{(2\pi)^2} \int d^2k\, k\, e^{-k\gamma}\, e^{-i\mathbf{k}\cdot(\mathbf{r}-\mathbf{r}')}, \quad (6)$$

where $\mathbf{k}$ is the variable conjugate to $\mathbf{r} - \mathbf{r}'$, and $k = |\mathbf{k}|$. The interlayer interaction energy then reads

$$E_{\text{I}}[\rho] = -\frac{C_{\text{dd}}}{2} \int d^2r\, \rho_1(\mathbf{r}) \int d^2r'$$
$$\times \int \frac{d^2k}{(2\pi)^2} k\, e^{-k\gamma}\, e^{-i\mathbf{k}\cdot(\mathbf{r}-\mathbf{r}')} \rho_2(\mathbf{r}'), \quad (7)$$

which bears a striking resemblance to the nonlocal HF interaction energy $E_{\text{dd}}^{(2)}$ for the *single-layer* system. Indeed, recall that [17,18]

$$E_{\text{dd}}^{(2)}[\rho] = -\frac{C_{\text{dd}}}{4} \int d^2r\, \rho(\mathbf{r}) \int d^2r'$$
$$\times \int \frac{d^2k}{(2\pi)^2} k\, e^{-i\mathbf{k}\cdot(\mathbf{r}-\mathbf{r}')} \rho(\mathbf{r}'). \quad (8)$$

Equation (8) corresponds exactly to the fourth term in Eq. (2) provided we use the definition $\lambda(\mathbf{r}) = \sqrt{4\pi\rho(\mathbf{r})}$. Now, comparing Eq. (7) to Eq. (8), we observe that $E_{\text{dd}}^{(2)}$ for the *single-layer* system can evidently be obtained (aside from a factor of 2) by simply evaluating the direct interaction between two 2D layers separated by a distance γ, and then taking the $\gamma \rightarrow 0$ limit. In order to understand this result, let us rewrite Eq. (4) as

$$E_{\text{I}}[\rho] = \int d^2r\, V_2(\mathbf{r})\rho_1(\mathbf{r}), \quad (9)$$

where

$$V_2(\mathbf{r}) = \int d^2r'\, \rho_2(\mathbf{r}')V_{\text{I}}(\mathbf{r} - \mathbf{r}'; \gamma) \quad (10)$$

can be thought of as the potential produced by $\rho_2(\mathbf{r})$. We see that if $\rho_2(\mathbf{r}) = \rho_0$ is uniform, then $V_2(\mathbf{r}) = 0$, meaning that $E_{\text{I}} = 0$ regardless of the form of $\rho_1(\mathbf{r})$. Thus, it is only the deviations from the uniform density ρ_0 which contribute to the interlayer interaction. Now, as we take $\gamma \rightarrow 0$, one can think of E_{I} as being the interaction energy between density fluctuations of two independent gases superposed on each other. With these comments in mind, an interesting interpretation of $E_{\text{dd}}^{(2)}$ develops; namely, $E_{\text{dd}}^{(2)}$ represents the classical *self-interaction* energy between density fluctuations in the gas of a *single-layer* 2D dFG. Viewing $E_{\text{dd}}^{(2)}$ in this way also naturally explains the factor of 2 mentioned above, in that we now have the relationship

$$E_{\text{dd}}^{(2)} = \frac{1}{2} \lim_{\gamma \rightarrow 0} E_{\text{I}}, \quad (11)$$

where the $\gamma \rightarrow 0$ limit is taken after the integration, since Eq. (4) is not convergent for $\gamma = 0$. In this sense, for a single 2D dFG, γ is simply a parameter which causes the divergent bare dipolar self-interaction energy integral to converge, after which one can set $\gamma = 0$. The connection displayed in Eq. (11) does not appear to have been noticed before, and provides an alternative route to obtaining the interaction energy functional (within the HF approximation) for a weakly modulated 2D dFG. In what follows, we shall make use of Eq. (11) to immediately construct the interlayer energy E_{I} without having to perform any additional calculations.

We are now in a position to write the total energy functional for the bilayer (BL) 2D dFG, namely,

$$E_{\text{BL}}[\lambda(\mathbf{r})] = E_{\text{SL}}[\lambda(\mathbf{r})] + E_{\text{I}}[\lambda(\mathbf{r})] = \frac{1}{16\pi} \frac{\hbar^2}{Mr_0^4} \int d^2r\, \lambda(\mathbf{r})^4 + \frac{\lambda_{\text{vW}}}{8\pi} \frac{\hbar^2}{Mr_0^2} \int d^2r\, |\nabla\lambda(\mathbf{r})|^2 + \frac{8}{45\pi^2} \frac{\hbar^2}{Mr_0^4} \int d^2r\, \lambda(\mathbf{r})^5$$
$$- \frac{C_{\text{dd}}}{4(4\pi)^2 r_0^4} \int d^2r\, \lambda(\mathbf{r})^2 \int d^2r' \int \frac{d^2k}{(2\pi)^2} k\, e^{-i\mathbf{k}\cdot(\mathbf{r}-\mathbf{r}')} \lambda(\mathbf{r}')^2$$
$$- \frac{1}{32\pi} \frac{\hbar^2}{Mr_0^4} \int d^2r\, \lambda(\mathbf{r})^6 \ln\left(1 + \frac{1}{a\sqrt{\lambda(\mathbf{r})} + b\lambda(\mathbf{r}) + c\lambda(\mathbf{r})^{\frac{3}{2}}}\right)$$
$$- \frac{C_{\text{dd}}}{2(4\pi)^2 r_0^4} \int d^2r\, \lambda_1(\mathbf{r})^2 \int d^2r' \int \frac{d^2k}{(2\pi)^2} k\, e^{-k\gamma}\, e^{-i\mathbf{k}\cdot(\mathbf{r}-\mathbf{r}')} \lambda_2(\mathbf{r}')^2. \quad (12)$$

A few comments are in order at this point. First, note that in Eq. (12), we have ignored the thickness of the layers and have prohibited the possibility of tunneling between the layers. In addition, while $E_{\text{BL}}[\lambda]$ does contain the intralayer correlations, we have not taken into account the interlayer correlations; in the absence of any QMC calculations for the bilayer geometry, this is an unavoidable approximation. Nevertheless,

we expect that omitting the interlayer correlations should not qualitatively affect the outcome of this work, since it is the intralayer correlations which largely determine the transition from the liquid-to-ordered state [1,16].

Following the methodology of the single-layer case, we will now investigate if the bilayer 2D dFG has a propensity to possess ordered states by employing Eq. (3), but now with

$E_{\mathrm{BL}}[\lambda]$ replacing $E_{\mathrm{SL}}[\lambda]$,

$$
\begin{aligned}
\Delta\varepsilon_{\mathrm{BL}} &= \frac{E_{\mathrm{BL}}[\lambda(\mathbf{r})] - E_{\mathrm{BL}}[\lambda_0]}{\int d^2 r \rho_0}\left(\frac{\hbar^2}{Mr_0^2}\right)^{-1} \\
&= \frac{E_{\mathrm{SL}}[\lambda(\mathbf{r})] - E_{\mathrm{SL}}[\lambda_0]}{\int d^2 r \rho_0}\left(\frac{\hbar^2}{Mr_0^2}\right)^{-1} \\
&\quad + \frac{E_{\mathrm{I}}[\lambda(\mathbf{r})]}{\int d^2 r \rho_0}\left(\frac{\hbar^2}{Mr_0^2}\right)^{-1} \\
&= \Delta\varepsilon_{\mathrm{SL}} + \Delta\varepsilon_{\mathrm{I}}, \quad (13)
\end{aligned}
$$

where we have made use of the fact that $E_{\mathrm{I}}[\lambda_0] = 0$. We will provide details for density modulations corresponding to the 1DSP and TWC in each layer, noting that other crystalline symmetries follow exactly the same analysis.

A. Density modulation for a 1DSP

The simplest *ansatz* corresponding to a 1D spatial modulation, with wave vector $\mathbf{q}$, is given by

$$
\rho(\mathbf{r}) = \rho_0[1 + \alpha\cos(\mathbf{q}\cdot\mathbf{r})], \quad (14)
$$

where $\alpha \ll 1$ represents the small amplitude deviation about the uniform density ρ_0, and is not to be interpreted as a variational parameter. Equation (14) can also be cast in terms of the dimensionless quantity $\lambda(\mathbf{r})$, viz.,

$$
\lambda(\mathbf{r}) = \lambda_0[1 + \alpha\cos(\mathbf{q}\cdot\mathbf{r})]^{\frac{1}{2}}. \quad (15)
$$

In the case of two layers, we should also take into account the possibility that the modulated densities are not commensurate, namely, that they may be offset relative to each other by some phase shift ϕ, viz.,

$$
\rho_1(\mathbf{r}) = \rho_0[1 + \alpha\cos(\mathbf{q}\cdot\mathbf{r})], \quad (16)
$$

$$
\rho_2(\mathbf{r}') = \rho_0[1 + \alpha\cos(\mathbf{q}\cdot\mathbf{r}' + \phi)]. \quad (17)
$$

Using Eqs. (16) and (17) in Eq. (7), we obtain for $\Delta\varepsilon_{\mathrm{I}}$,

$$
\Delta\varepsilon_{\mathrm{I}} = -\frac{1}{4}\alpha^2 \tilde{q}\, e^{-\tilde{\gamma}\tilde{q}} \lambda_0^2 \cos(\phi), \quad (18)
$$

where we have introduced the dimensionless quantities $\tilde{q} = qr_0$ and $\tilde{\gamma} = \gamma/r_0$. Note that $\Delta\varepsilon_{\mathrm{I}}$ vanishes when $\gamma \to \infty$, or when the stripe phases in the layers are shifted by $\phi = \pi/2\bmod(2\pi)$. Regardless, it is clear that Eq. (18) favors the situation in which the stripes in each layer are commensurate, viz., $\phi = 0$. Our prediction that the 1DSP in each layer are in phase is supported by the other calculations [5,8,9,14,15], although our determination is obtained via a simple analytical expression, Eq. (18), rather than relying on involved numerical computations.

Coming back to Eq. (13), we now make use of the fact that $\alpha \ll 1$, so that a perturbative approach is sensible, meaning that we need only consider shifts to $O(\alpha^2)$. It is evident from Eq. (18) that the shift from the interlayer interaction is already

$O(\alpha^2)$. Utilizing the result for $\Delta\varepsilon_{\mathrm{SL}}$ from Ref. [1],

$$
\begin{aligned}
\frac{\Delta\varepsilon_{\mathrm{SL}}}{\alpha^2} &= \frac{1}{8}\lambda_0^2 + \lambda_{\mathrm{vW}}\frac{\tilde{q}^2}{16} + \left[\frac{2}{3\pi} - \frac{1}{8}\frac{\tilde{q}}{\lambda_0}\right]\lambda_0^3 \\
&\quad - \frac{1}{8}\lambda_0^4\left[\frac{3}{2}\ln[f_0] + \frac{11}{16}\lambda_0 A + \frac{1}{16}\lambda_0^2 B\right], \quad (19)
\end{aligned}
$$

where

$$
f(\lambda) = \left(1 + \frac{1}{a\sqrt{\lambda} + b\lambda + c\lambda^{\frac{3}{2}}}\right), \quad (20)
$$

$$
f_0 \equiv f(\lambda_0),\ \ f_0' \equiv \left.\frac{df}{d\lambda}\right|_{\lambda=\lambda_0},\ \ f_0'' \equiv \left.\frac{d^2 f}{d\lambda^2}\right|_{\lambda=\lambda_0}, \quad (21)
$$

$$
A = \frac{f_0'}{f_0}, \quad (22)
$$

$$
B = \frac{f_0'' f_0 - f_0'^2}{f_0^2}, \quad (23)
$$

we finally obtain our desired result:

$$
\begin{aligned}
\frac{\Delta\varepsilon_{\mathrm{BL}}^{\mathrm{1DSP}}}{\alpha^2} &= \frac{1}{8}\lambda_0^2 + \lambda_{\mathrm{vW}}\frac{\tilde{q}^2}{16} + \left[\frac{2}{3\pi} - \frac{1}{8}\frac{\tilde{q}}{\lambda_0}\right]\lambda_0^3 \\
&\quad - \frac{1}{8}\lambda_0^4\left[\frac{3}{2}\ln[f_0] + \frac{11}{16}\lambda_0 A + \frac{1}{16}\lambda_0^2 B\right] \\
&\quad - \frac{1}{4}\tilde{q}\, e^{-\tilde{\gamma}\tilde{q}} \lambda_0^2. \quad (24)
\end{aligned}
$$

Recall that all energies are scaled by $\hbar^2/Mr_0^2$, and observe that the right-hand side of Eq. (24) has no dependence on α, emphasizing that α is not a variational parameter in our analysis. Equation (24) illustrates that the interlayer interaction will actually enhance the system's tendency to undergo a transition to a 1DSP because it contributes a negative component to the energy shift $\Delta\varepsilon_{\mathrm{BL}}^{\mathrm{1DSP}}$. Indeed, it was found in Ref. [1] that a negative contribution to the energy shift [arising from the nonlocal HF interaction, Eq. (8)], was essential for the single-layer system to undergo a phase transition. The additional term coming from Eq. (18) will clearly serve to lower the system's energy in favor of an inhomogeneous state in the bilayer configuration, and therefore *lower* the coupling λ_0 required for the onset of the phase transition.

B. Density modulation for a triangular Wigner crystal

To find the expression for $\Delta\varepsilon_{\mathrm{BL}}$ corresponding to a triangular TWC, we use the densities [1,20]

$$
\begin{aligned}
\rho(\mathbf{r}) = \rho(x,y) = \rho_0\Bigg[&\sqrt{1 - \frac{3}{2}\alpha^2} + \alpha\cos(qx) \\
&+ 2\alpha\cos\left(\frac{q}{2}x\right)\cos\left(\frac{\sqrt{3}}{2}qy\right)\Bigg]^2, \quad (25)
\end{aligned}
$$

$$
\begin{aligned}
\lambda(\mathbf{r}) = \lambda(x,y) = \lambda_0\Bigg[&\sqrt{1 - \frac{3}{2}\alpha^2} + \alpha\cos(qx) \\
&+ 2\alpha\cos\left(\frac{q}{2}x\right)\cos\left(\frac{\sqrt{3}}{2}qy\right)\Bigg], \quad (26)
\end{aligned}
$$

in each layer, with the understanding that the spatial coordinates are specific to a given layer. In view of our findings

from the 1DSP case, we do not need to consider a scenario in which the TWC lattices in the two layers are staggered in any way (it is in this sense that we mean the TWCs in each layer are commensurate). This is in contrast to the Coulomb bilayer problem, where the lattices in each layer must be incommensurate in order to minimize the total energy of the system [16].

From Ref. [1] we have for the single layer

$$\frac{\Delta \varepsilon_{\text{SL}}}{\alpha^2} = \frac{3}{2} \lambda_0^2 + \lambda_{\text{vW}} \frac{3\tilde{q}^2}{4} + \left[\frac{8}{\pi} - \frac{3}{2} \frac{\tilde{q}}{\lambda_0} \right] \lambda_0^3$$
$$- \frac{1}{4} \lambda_0^4 \left[9 \ln[f_0] + \frac{33}{8} \lambda_0 A + \frac{3}{8} \lambda_0^2 B \right]. \quad (27)$$

As previously shown, with no additional effort we can make use of the connection between E_{I} and $E_{\text{dd}}^{(2)}$ to write

$$\frac{\Delta \varepsilon_{\text{I}}}{\alpha^2} = -3\tilde{q} \, e^{-\tilde{q}\tilde{\gamma}} \lambda_0^2, \quad (28)$$

which leads directly to

$$\frac{\Delta \varepsilon_{\text{BL}}^{\text{TWC}}}{\alpha^2} = \frac{3}{2} \lambda_0^2 + \lambda_{\text{vW}} \frac{3\tilde{q}^2}{4} + \left[\frac{8}{\pi} - \frac{3}{2} \frac{\tilde{q}}{\lambda_0} \right] \lambda_0^3$$
$$- \frac{1}{4} \lambda_0^4 \left[9 \ln[f_0] + \frac{33}{8} \lambda_0 A + \frac{3}{8} \lambda_0^2 B \right] - 3\tilde{q} \, e^{-\tilde{q}\tilde{\gamma}} \lambda_0^2. \quad (29)$$

Armed with expressions for the shifts for both the 1DSP, Eq. (24), and a TWC, Eq. (29), we are now poised to investigate the phase diagram for the bilayer 2D dipolar Fermi gas.

III. PHASE DIAGRAM OF THE BILAYER SYSTEM

In contrast to the single-layer problem, there are now two independent variables which may be varied, namely, the coupling λ_0 and the separation between the two layers γ. Consequently, our phase diagram will be an exploration of how the system responds to changes in these two variables. As discussed in Ref. [1], for the 1DSP, we take $\tilde{q} = 2\lambda_0$, while for the TWC we set $\tilde{q} = (8\pi/\sqrt{3})^{1/2}\lambda_0/2$. The value $\tilde{q} = 2\lambda_0$ is the wave vector associated with the lowest energy for the formation of the stripe phase, while $\tilde{q} = (8\pi/\sqrt{3})^{1/2}\lambda_0/2$ for the TWC enforces that we have only one atom per unit cell.

Specifically, we look for a change in the signs of $\Delta \varepsilon_{\text{BL}}^{\text{1DSP}}/\alpha^2$ and $\Delta \varepsilon_{\text{BL}}^{\text{TWC}}/\alpha^2$ as we vary λ_0 for a fixed layer separation, γ. As it happens, $\Delta \varepsilon_{\text{BL}}^{\text{1DSP}}/\alpha^2$ *always* crosses zero first (indicating that the 1DSP phase is now energetically favorable over the uniform state) while $\Delta \varepsilon_{\text{BL}}^{\text{TWC}}/\alpha^2$ remains positive. Then, as λ_0 is further increased, $\Delta \varepsilon_{\text{BL}}^{\text{TWC}}/\alpha^2$ also crosses zero (i.e., becomes negative), and we determine the preferred inhomogeneous phase by comparing the values of $\Delta \varepsilon_{\text{BL}}^{\text{1DSP}}/\alpha^2$ and $\Delta \varepsilon_{\text{BL}}^{\text{TWC}}/\alpha^2$; if $\Delta \varepsilon_{\text{BL}}^{\text{TWC}}/\alpha^2 < \Delta \varepsilon_{\text{BL}}^{\text{1DSP}}/\alpha^2$, the TWC phase is the ordered state, even though both phases are lower in energy than the uniform Fermi liquid. The procedure is repeated for different layer separations, leading to the phase diagram shown in Fig. 1. It should be noted that owing to the fact that the liquid, 1DSP, and TWC belong to different symmetry classes, our ordered states are separated by first-order phase transitions.

Let us now take a closer look at Fig. 1. First, we observe that for values of $\tilde{\gamma} = \gamma/r_0 \gtrsim 4$, the layers are effectively

uncoupled, and the results of Ref. [1] are recovered, viz., the system undergoes a transition first to a 1DSP followed by a TWC at higher coupling. Next, consider the case where we have a fixed layer separation $\tilde{\gamma}$ and start with small λ_0, which increases as we move up vertically in the phase diagram. It is evident that the window in which the 1DSP precedes the TWC gets smaller and smaller as the fixed layer separation decreases. Indeed, for say $\tilde{\gamma} = 0.5$, the range of λ_0 distinguishing the 1DSP from the TWC is very narrow. This is perhaps not so surprising given that the $\Delta \varepsilon_{\text{I}}$ contribution has a maximum negative component as $\tilde{\gamma} \to 0$.

If we now fix the coupling, λ_0, and move horizontally in the phase diagram (i.e., varying $\tilde{\gamma}$), we see that there are layer separations at which a crystal or 1DSP is the preferred phase. For example, if we take $\lambda_0 = 1$, and move horizontally in our phase diagram starting from small $\tilde{\gamma}$, we observe that up to $\tilde{\gamma} \approx 1$, each layer possesses a TWC as the ground state of the system. The system then undergoes a transition to a 1DSP, which lasts over only a very short coupling range, followed by the system melting to a liquid. Looking now at values of $1.4 \lesssim \lambda_0 \lesssim 1.5$, we see that the liquid state is never present, and the system goes from a 1DSP to a TWC as the layer separation is decreased (i.e., moving right to left in the phase diagram). Finally, notice that for $\lambda_0 \gtrsim 1.5$, each layer remains frozen in a TWC, regardless of the layer separation $\tilde{\gamma}$.

We have performed the same analysis as above for other crystal symmetries, e.g., square, rhombic, and rectangular, and have confirmed that none of these crystal symmetries are more energetically favorable than the TWC. This finding is in stark contrast to a bilayer 2D electron system [16], where depending on the coupling and layer separation, the TWC is *not* necessarily the ground state of the system. It appears that, at least within our DFT, the only two phases possessed by the bilayer 2D dFG are the 1DSP and the TWC.

Before closing this section, it is worthwhile briefly commenting on the feasibility of experimentally exploring our phase diagram. We note that it will in fact be difficult to reach strong enough interactions (or high enough densities) with ^{161}Dy ($d \sim 10\mu_B$) or other magnetic atoms. Specifically, for ^{161}Dy, typically $\lambda_0 < 1$, implying that it will be difficult to observe the density instabilities with magnetic atoms, in either a single-layer geometry, or equivalently, the large γ/r_0 sector of our phase diagram. In contrast, dipolar molecules with an electric dipole moment should allow experiments to reach sufficiently strong interactions to observe the 1DSP or TWC. For example, using ^{23}Na ^{40}K molecules, with dipole moments of up to ~ 2.7 Debye, current experimental conditions [21] should allow $\lambda_0 \sim 1.4$, which is within the range of coupling in our phase diagram where the Fermi liquid state is completely absent for any layer separation. Our phase diagram suggests that it should be easier to experimentally investigate density instabilities in bilayer configurations because the transition from the Fermi liquid to the ordered state occurs at lower coupling as the spacing between the layers, γ/r_0, is decreased. This is important from an experimental point of view if one wishes to work with chemically inactive ^{161}Dy atoms, where $\lambda_0 < 1$. According to our phase diagram, the bilayer geometry still allows the observation of a phase transition for $\lambda_0 < 1$ by varying the interlayer separation. However, for ^{161}Dy, $r_0 \sim 0.02 \, \mu$m, meaning that layer separations,

$\gamma \sim 0.02 \ \mu$m, would have to be readily achievable in the laboratory. It therefore appears that the most promising candidate for experimentally exploring our phase diagram is by using ^{23}Na ^{40}K molecules, where both the 1DSP and TWC phases should be readily accessible [21].

IV. CONCLUSIONS AND CLOSING REMARKS

We have extended the density-functional theory of Ref. [1] to the case of a bilayer, two-dimensional dipolar Fermi gas. The present density-functional study investigates the possibility of a quantum phase transition to either a stripe or a Wigner crystal phase in the bilayer two-dimensional dipolar Fermi gas. While developing our formal extension of the work in Ref. [1], we have found an interesting connection between the direct interlayer interaction energy, Eq. (7), and the *nonlocal* Hartree-Fock energy, Eq. (8); namely, that the nonlocal Hartree-Fock energy can be obtained by considering the direct interaction between two different layers, separated by a distance γ, and then taking the $\gamma \to 0$ limit. We have provided a physical interpretation of this connection, which is that $E_{\text{dd}}^{(2)}$ represents the classical self-interaction energy in an inhomogeneous two-dimensional dipolar Fermi gas. We have also presented analytical expressions, Eqs. (24) and (29), which allow a numerically efficient examination of the phase diagram for the bilayer system. The relative ease of obtaining the phase diagram for the bilayer system should be viewed as a testament to the utility of the density-functional theory approach.

Our phase diagram (see Fig. 1) demonstrates that the bilayer two-dimensional dipolar Fermi gas has only two energetically favorable inhomogeneous phases, viz., a one-dimensional stripe phase or a triangular Wigner crystal in each layer. In contrast to the case of the bilayer electron system (see Ref. [16]), the stripe and Wigner crystal phases are perfectly commensurate in the two layers, with no possibility of other crystalline symmetry phases existing owing to their high energy cost relative to the triangular Wigner crystal. Through an exploration of the $(\tilde{\gamma}, \lambda_0)$ space, we have also confirmed that there are coupling regimes for which the system is always in a Wigner crystal or stripe phase, completely bypassing the liquid state, regardless of the separation between the layers. We have also shown that the range of coupling, λ_0, over which the phase transition occurs can be significantly reduced in a bilayer geometry, and have provided a simple explanation for this result in terms of the connection between the nonlocal Hartree-Fock and interlayer interaction energy terms.

To close this paper, we mention that an interesting progression of this work would be to consider other exotic Fermi systems, such as the electron-hole bilayer problem [22–24], which to date has not been studied within a density-functional theory approach. It is also still an outstanding problem to provide a density-functional theory in the case where the dipole moments of the atoms are canted at some angle relative to the z axis (i.e., taking into account the full anisotropic nature of the dipole-dipole interaction). Finally, the development of our density-functional theory to finite temperatures would be of interest, because it is expected that at nonzero temperatures, the physics of the Berezinskii-Kosterlitz-Thouless transition [25] is the appropriate description of the system.

[1] B. P. van Zyl, W. Kirkby, and W. Ferguson, Phys. Rev. A **92**, 023614 (2015).

[2] R. M. Dreizler and E. K. U. Gross, *Density Functional Theory: An Approach to the Quantum Many-Body Problem* (Springer-Verlag, Berlin, 1990).

[3] K. Sun, C. Wu, and S. Das Sarma, Phys. Rev. B **82**, 075105 (2010).

[4] Y. Yamaguchi, T. Sogo, T. Ito, and T. Miyakawa, Phys. Rev. A **82**, 013643 (2010).

[5] N. T. Zinner and G. M. Bruun, Eur. J. Phys. **65**, 133 (2011).

[6] M. M. Parish and F. M. Marchetti, Phys. Rev. Lett. **108**, 145304 (2012).

[7] L. M. Sieberer and M. A. Baranov, Phys. Rev. A **84**, 063633 (2011).

[8] J. K. Block, N. T. Zinner, and G. M. Bruun, New J. Phys. **14**, 105006 (2012).

[9] M. Babadi and E. Demler, Phys. Rev. B **84**, 235124 (2011).

[10] J. K. Block and G. M. Bruun, Phys. Rev. B **90**, 155102 (2014).

[11] M. Babadi, B. Skinner, M. M. Fogler, and E. Demler, Europhys. Lett. **103**, 16002 (2013).

[12] N. Matveeva and S. Giorgini, Phys. Rev. Lett. **109**, 200401 (2012).

[13] S. H. Abedinpour, R. Asgari, B. Tanatar, and M. Polini, Ann. Phys. (NY) **340**, 25 (2014).

[14] F. M. Marchetti and M. M. Parish, Phys. Rev. B **87**, 045110 (2013).

[15] M. Callegari, M. M. Parish, and F. M. Marchetti, arXiv:1601.06988.

[16] G. Goldoni and F. M. Peeters, Europhys. Lett. **37**, 293 (1997).

[17] B. Fang and B.-G. Englert, Phys. Rev. A **83**, 052517 (2011).

[18] B. P. van Zyl, E. Zaremba, and P. Pisarski, Phys. Rev. A **87**, 043614 (2013).

[19] N. Choudhury and S. K. Ghosh, Phys. Rev. B **51**, 2588 (1995).

[20] Note that we have not included the "granular density" analysis discussed in Ref. [1] when exploring the triangular Wigner crystal phase. The granular density analysis does not qualitatively alter the phase diagram obtained from the simpler perturbative approach presented in this paper.

[21] J. W. Park, S. A. Will, and M. W. Zwierlein, Phys. Rev. Lett. **114**, 205302 (2015).

[22] G. Senatore and S. De Palo, Contrib. Plasma Phys. **43**, 363 (2003).

[23] J. Ye, J. Low Temp. Phys. **158**, 882 (2009).

[24] J. Schleede, A. Filinov, M. Bonitz, and H. Fehske, Contrib. Plasma Phys. **52**, 819 (2012).

[25] V. L. Berezinskii, Zh. Eksp. Teor. Fiz. **61**, 1144 (1971) [Sov. Phys. JETP **34**, 610 (1972)]; J. M. Kosterlitz and D. J. Thouless, J. Phys. C **7**, 1046 (1974).